



This open access document is published as a preprint in the Beilstein Archives with doi: 10.3762/bxiv.2020.47.v1 and is considered to be an early communication for feedback before peer review. Before citing this document, please check if a final, peer-reviewed version has been published in the Beilstein Journal of Nanotechnology.

This document is not formatted, has not undergone copyediting or typesetting, and may contain errors, unsubstantiated scientific claims or preliminary data.

Preprint Title Microwave photon detection by an Al Josephson junction

Authors Leonid S. Revin, Andrey L. Pankratov, Anna V. Gordeeva, Anton A. Yablokov, Igor V. Rakut, Victor O. Zbrozhek and Leonid S. Kuzmin

Publication Date 09 Apr 2020

Article Type Full Research Paper

ORCID® iDs Andrey L. Pankratov - <https://orcid.org/0000-0003-2661-2745>;
Leonid S. Kuzmin - <https://orcid.org/0000-0002-8051-484X>

1 **Microwave photon detection by an Al Josephson junction**

2 Leonid S. Revin^{*1,2}, Andrey L. Pankratov^{1,2,3}, Anna V. Gordeeva², Anton A. Yablokov^{1,2}, Igor V.
3 Rakut^{2,3}, Victor O. Zbrozhek² and Leonid S. Kuzmin^{2,4}

4 Address: ¹Institute for Physics of Microstructures of RAS, GSP-105, Nizhny Novgorod, 603950,
5 Russia; ²Center of Cryogenic Nanoelectronics, Nizhny Novgorod State Technical University,
6 Nizhny Novgorod, Russia; ³Lobachevsky State University of Nizhny Novgorod, Nizhny Novgorod,
7 Russia and ⁴Chalmers University of Technology, SE-41296 Gothenburg, Sweden

8 Email: Leonid S. Revin - rls@ipmras.ru

9 * Corresponding author

10 **Abstract**

11 The aluminum Josephson junction (JJ) with a critical current, suppressed by a factor of three com-
12 paring with the maximal value calculated from the gap, is experimentally investigated for appli-
13 cation as a threshold detector of microwave photons. We present the preliminary results of mea-
14 surements of the lifetime of the superconducting state and the probability of switching by 9 GHz
15 external signal. We found an anomalously large lifetime, not described by the Kramers' theory
16 for the escape time over a barrier under the influence of fluctuations. We explain it by the phase
17 diffusion regime, which is evident from the temperature dependence of the switching current his-
18 tograms. Therefore, the phase diffusion allows to significantly improve the noise immunity of a
19 device, radically decreasing the dark count rate, but it will also decrease the single photon sensitiv-
20 ity of the considered threshold detector. Quantization of the switching probability tilt versus signal
21 attenuation for various bias currents through the JJ is observed, which resembles the differentiation
22 between N and $N + 1$ photon absorption.

23 **Keywords**

24 Josephson junction; switching current distribution; phase diffusion; photon counter

25 Introduction

26 Currently, an important problem is the creation of single-photon counters in the GHz frequency
27 range. Such devices are in demand in several areas, such as the search for axions, the alleged parti-
28 cles of dark matter [1-3] and quantum computing [4]. Commercially available single-photon detec-
29 tors operate at frequencies of hundreds of THz and higher [5,6]. For the lower frequency range, a
30 new class of single microwave photon detectors is needed. In this regard, a current-biased Joseph-
31 son junction is of particular interest for applications as a threshold detector since its phase dynam-
32 ics is altered even by a weak probe field. Rich dynamics of the JJ constantly inspires new applica-
33 tions, such as thermometry [7,8], noise statistics [9-11] and single photon detection [12].

34 There are, at least, two different approaches for practical realization of the single-photon detec-
35 tors based on Josephson junctions, both having their advantages and disadvantages. The first ap-
36 proach relies on a continuous current sweep at a constant repetition rate and the measurements of
37 the switching current distributions, from which the response and sensitivity can be determined [13-
38 15]. In particular, in [15] the tunneling properties of the current-biased Josephson junction coupled
39 with a resonator directly depend on the number of microwave photons in the resonator. The main
40 disadvantages of this approach are the long initialization and freezing times of the detector. The
41 detector works by slowly increasing the bias current from zero. This ramp takes seconds to avoid
42 non-adiabatic excitation in a JJ. As soon as the detector switches, it must be reset by setting the cur-
43 rent back to zero and waiting when a Josephson phase relaxes in a potential well. This implies a
44 low repetition rate.

45 The second approach for experimental microwave detection [16,17] uses the switching events of the
46 biased Josephson junction resulting from a single absorption. In contrast to the previous approach,
47 this one requires less downtime of the detector, determined by the biasing time to the desired cur-
48 rent only. However, the operation in this mode does not provide information on the number of
49 absorbed photons and only above-threshold signals can be detected. Also, a special care must be
50 taken to minimize the false switching events of the detector due to thermal fluctuations and macro-
51 scopic quantum tunneling.

52 In this article the second approach is used in application to a prototype of a single photon counter
53 described in [3]. We study the possibility of detecting photons of GHz frequency range using and
54 aluminum Josephson junction with a suppressed critical current. The main requirement to the such
55 counter is an extremely large lifetime (thousand of seconds), orders of magnitude larger than the
56 switching time after the photon absorption (typically less than nanoseconds). In [3] it was shown
57 theoretically that both the required sensitivity and the noise immunity can be reached at the same
58 time in JJ with a suppressed critical current. Besides that, the mesoscopic junctions with low crit-
59 ical currents have received a great deal of interest by themselves, since they exhibit such a phe-
60 nomenon as the diffusion of the Josephson phase [18-21].

61 The Josephson phase diffusion in small junctions has been studied both experimentally [22,23]
62 and theoretically [24]. Recently, this regime has been observed also in layered high-temperature
63 superconductors [25]. The significance of this effect depends on the ratio of thermal fluctuations
64 kT , the damping parameter α and the Josephson energy E_J . Here we will consider a small tunnel
65 junction with the thermal noise intensity of $\gamma = k_B T / E_J \geq 2 \cdot 10^{-2}$ and $\alpha > 0.1$, and show
66 experimentally an unusually large lifetime of the superconducting state, which we attribute to the
67 phase diffusion according to [19]. The increase of the lifetime of the superconducting state due
68 to the phase diffusion was also observed in [26] for the similar conditions. On the other hand the
69 phase diffusion is expected to decrease the sensitivity to single photons for the same reason that it
70 improves the noise immunity. To our knowledge so far there are no works dedicated to the role of
71 the of phase diffusion in the response to single photons. In the last section of the article we show
72 the experimental measurements of the switching probability induced by weak microwave signal
73 and discuss some features of the measured response, which may indicate the sensitivity to several
74 photon bunches.

75 The analysis of the phase-diffusion phenomena is a special case of a general problem of the motion
76 of a Brownian particle in a washboard potential in the framework of the resistively-capacitively
77 shunted junction (RCSJ) model for the dynamics of the Josephson phase [27,28]. The tilt of the
78 washboard potential is controlled by the bias current I and is defined as $E_J(I/I_C)$, where I_C is the

79 critical current and $E_J = \hbar I_C / 2e$. The particle moves along the potential in the presence of friction,
80 whose strength is characterized by $\alpha = \omega_p / \omega_c$, where $\omega_p = (2eI_C / \hbar C)^{1/2}$ is the plasma frequency,
81 $\omega_c = 2eI_C R_N / \hbar$ is the characteristic frequency, R_N is the normal state resistance and C is the ca-
82 pacitance.

83 The superconducting state of the JJ corresponds to the rest of the particle in one well of the poten-
84 tial. The exit from this metastable state corresponds to the appearance of the finite voltage at the
85 junction. In the case of low damping (but depending also on the barrier height and noise inten-
86 sity), the particle, jumping over the barrier, gains enough energy to move along the potential in the
87 running state. While if the damping α is sufficiently large, the escape due to the thermal or quan-
88 tum fluctuations does not necessarily lead to the running state appearance. After an escape event,
89 the particle can move down the potential for several wells and then relax into one of the potential
90 minima [22]. When the barrier and noise are large, the exit from the well and the subsequent re-
91 trapping processes may occur many times at a given bias current.

92 The most evident signature of the phase diffusion phenomenon is the temperature dependence of
93 the switching current distribution [20,29]. For underdamped junctions ($\alpha \ll 1$), the width of the
94 switching current distributions monotonically decreases with decreasing temperature. In the case
95 of moderately damped junctions ($\alpha > 0.2$) the switching dynamics changes due to the phase
96 diffusion: the width of the distribution decreases with increasing temperature. A change in the
97 sign of the derivative of the second moment of the distribution is a reliable indicator of retrapping
98 processes. Another sign of the phase diffusion is an increase in the lifetime of the superconduct-
99 ing state in comparison with the classical Kramers' theory [30,31]. The exit of the particle from
100 the well due to fluctuations does not lead to the instantaneous appearance of a final voltage at the
101 Josephson junction, which can be seen in experiment as an increase of the noise immunity of the
102 system.

103 The principle of operation of a single-photon counter based on the Josephson junction is the fol-
104 lowing: at the initial moment of time, the junction is in a superconducting state with bias current I
105 close to the critical one. In standby mode there is no voltage at the junction. An incoming external

106 signal from a photon (current oscillations) can change the state of the system by switching it to a
107 resistive state with a finite resistance value. At the same time the detector may be triggered spon-
108 taneously due to thermal fluctuations in the classical region of temperatures and tunneling through
109 the barrier in the quantum case [14,32].

110 **Experimental**

111 Following the line proposed in Ref. [3], the aluminum Al/AlO_x/Al tunnel junction $0.4 \times 2 \mu\text{m}^2$
112 was fabricated using a self-aligned shadow evaporation technique. Its current-voltage charac-
113 teristic shown in the inset of Fig. 1 has a well-defined hysteresis. The double voltage gap of the
114 junction is 0.38 mV, corresponding to the critical temperature of Al $T_C = 1.2$ K, the capacitance
115 is $C \approx 0.036$ pF, the critical current density is $3.8 \cdot 10^{-3}$ kA/cm² and the normal resistance is
116 $R_N = 2300 \Omega$, which gives the maximal possible value of the critical current $I_C^{max} = 1.764kT_C/eR_N$
117 around 80 nA. The measured critical current is $I_C = 28$ nA at the temperature of 20 mK. The
118 damping of the Josephson junction calculated for the measured I_C is $\alpha = 0.24$.

119 The sample was mounted in an rf-tight box with a superconducting shielding on the coldest plate of
120 Triton 200 dry dilution refrigerator. The dc-bias wires were filtered with feed-through capacitors at
121 the room temperature and RC filters at the 10 mK cryostat plate, minimizing the effect of unwanted
122 low-frequency noise. In order to avoid ground loops the measurement scheme was designed with a
123 single ground.

124 For the switching current measurements, the bias current of the junction was ramped up at a con-
125 stant rate of $\dot{I} = 5 \cdot 10^{-8}$ A/s. The voltage was measured using a low noise room-temperature
126 differential amplifier AD745 and was fed to a high-speed NI ADC-card. This signal was used to
127 trigger a fast record of the switching current value. Such a procedure was repeated at least $5 \cdot 10^3$
128 times at each temperature, and as a result the switching current histograms were compiled in the
129 temperature range between 1 K and 20 mK. For the lifetime measurements, the experimental setup
130 was the same, except that the bias current was set to a predetermined value during the 20 ms to pre-
131 vent particle excitation caused by a rapid decrease in the barrier, and remained constant until the

132 appearance of a gap voltage due to thermal noise or quantum tunneling. The lifetime measurements
 133 were repeated at least 200 times for each value of the bias current.

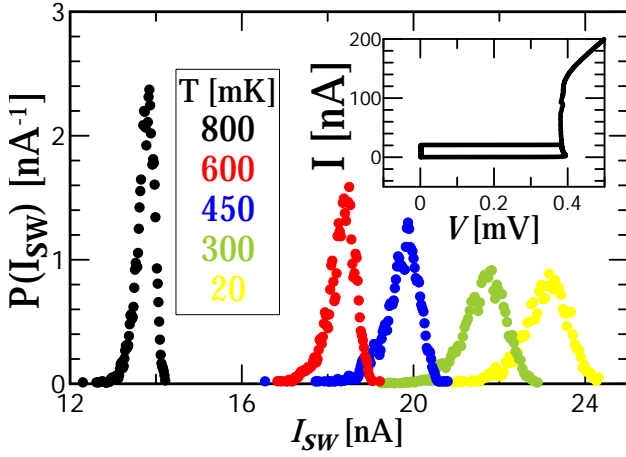


Figure 1: Experimentally measured histogram $P(I_{SW})$ of switching the Josephson junction to the resistive state for current I_{SW} at temperatures indicated from top to bottom for curves from left to right. The inset shows the I-V curve of the junction at 20 mK.

134 For a high-frequency experiment, a microwave signal was fed into the cryostat via a phosphor
 135 bronze twisted-pairs with attenuation of -15 dB per meter at 9 GHz and with a loop antenna near
 136 the JJ. The rf-signal from the external microwave synthesizer was attenuated using the voltage con-
 137 trolled room-temperature attenuator, preliminarily calibrated with a commercial spectrum analyzer.
 138 The high-frequency signal was varied from a high power at which the Shapiro steps and photon as-
 139 sisted tunneling steps are well pronounced at the IV-curve, to a low power whose presence can be
 140 observed only in the switching histograms and in the decrease of the superconducting state lifetime.

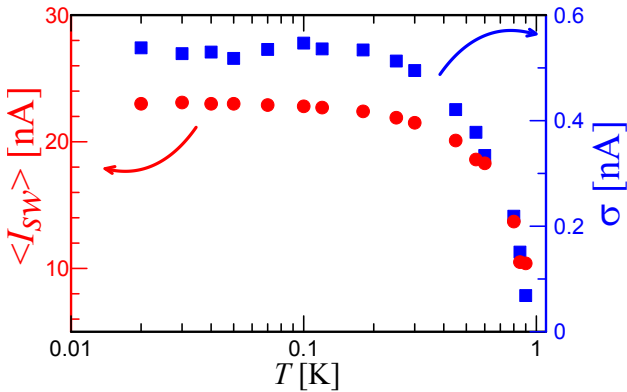


Figure 2: Temperature dependence of the mean switching current (left axis, red dots) and its standard deviation (right axis, blue squares).

141 Results and Discussion

142 In this section we present preliminary results of the first measurements. First, we assemble the
 143 switching current distributions (Fig. 1) and extract values for the mean switching current $\langle I_{SW} \rangle$
 144 and standard deviation σ , which are plotted in Fig. 2 for various temperatures of the chip. The de-
 145 crease of $\langle I_{SW} \rangle$ with temperature increase indicates that here the thermal activation of the phase is
 146 the main switching mechanism. At the temperatures below $T \approx 300$ mK there is a saturation both
 147 in $\langle I_{SW} \rangle$ and σ . The behavior of $\sigma(T)$ in the entire temperature range of the experiment shows the
 148 well-known signature of the phase diffusion, observed for example in [20,23,29].

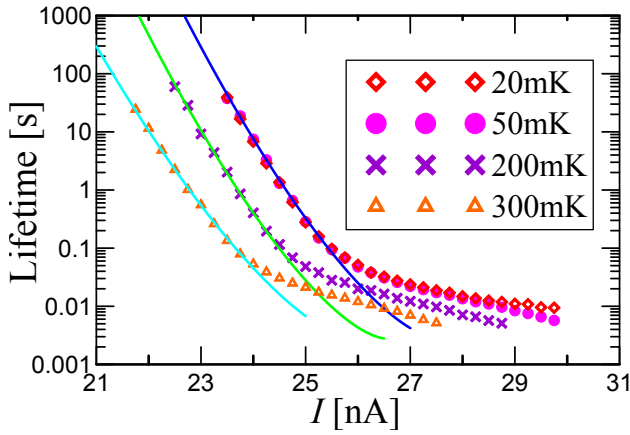


Figure 3: Experimental lifetimes as functions of bias current for various sample temperatures (symbols) and fitting by formula (1) (solid curves).

149 The presence of the phase diffusion also can explain the results of the lifetime (the inverse of the
 150 escape rate) measurements, shown in Fig. 3. The lifetime of the superconducting state corresponds
 151 to the mean time of dark counts of a single photon detector. We have measured the dependencies of
 152 the lifetime for various bias currents and temperatures and without high-frequency signal. One can
 153 see the linear slopes of the lifetime versus bias current for 2-3 orders of magnitude in a logarithmic
 154 scale, which means the exponential dependence of the lifetime versus potential barrier height. The
 155 plateau in the experimental points in Fig. 3 below 0.03 s is due to time constants of the measurement
 156 setup. To find out more about the switching conditions the experimental curves have been fitted by
 157 the Kramers' formula for the lifetime in the following form [28,30,31] (for the overdamped case,

158 see [33]):

$$159 \quad \tau = \frac{f(\alpha) \exp(\Delta u/\gamma)}{\sqrt{1-i^2}}, \quad (1)$$

160 where $i = I/I_C$ is the dimensionless bias current, $\Delta u = 2\sqrt{1-i^2} + i(2 \arcsin(i) - \pi)$ is the potential
161 barrier height and $\gamma = I_T/I_C$ is the noise intensity and $I_T = 2ek_B T/\hbar$ is the fluctuational current,
162 which can be calculated for a given temperature T as: $I_T[\mu\text{A}] = 0.042T[\text{K}]$ [27]. As well-known
163 [34], if the well and the barrier of a potential profile can be approximated by parabolas, then $f(\alpha)$
164 does not depend on the working temperature. However, for the range $\alpha \approx 1$, the exact prefactor
165 $f(\alpha)$ is unknown [31], therefore we use $f(\alpha)$ as a fitting parameter.

166 Substituting the temperature 300 mK into γ for our experimental parameters, one gets $\gamma = 0.48$.
167 For so large fluctuations the barrier height even with zero bias current is comparable with noise
168 intensity and the corresponding lifetime must be much smaller than measured in the experi-
169 ment. If we use γ as a fitting parameter together with $f(\alpha)$, we get the best fit for the following
170 parameters: $f(\alpha) = 0.00035$ seconds for all curves, $I_C = 26.5; 27; 28$ nA, noise intensity
171 $\gamma = 0.0137; 0.0112; 0.011$ for temperatures 300, 200, 50 mK, respectively. One can see that I_C
172 in this case corresponds to the measured values.

173 Thus, the comparison of measurements and fitting shows that the average time between dark counts
174 significantly exceeds the time predicted by Kramers' theory, with mean values reaching hundreds
175 of seconds and thousands of seconds in single measurements. If we believe, that it is the phase dif-
176 fusion regime significantly suppresses the dark count rate, the next important question is to figure
177 out how it influences the sensitivity to the photons. In order to do this we perform measurements of
178 the detection probability as a function of the attenuator voltage of 9 GHz photons in a 50 ms pulse,
179 incident on the sample area, for three values of bias current I , shown in Fig. 4.

180 Left vertical axis shows the experimental data i.e., the number of detector counts to the total num-
181 ber of pulses (200 pulses). The horizontal axis corresponds to the attenuation (output power) of
182 the external high-frequency signal. For high incident photon fluxes, the detector switches for all
183 200 pulses, i.e. counts all pulses. For smaller fluxes our experimental data show that for 2.5 orders

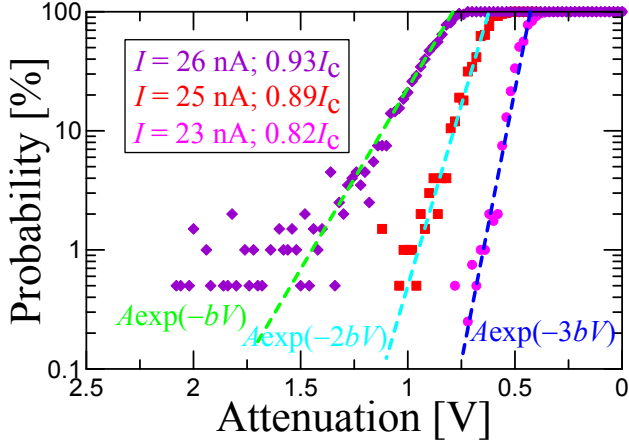


Figure 4: Detection probability of 9 GHz 50 ms pulses of different power (signal attenuation) for different values of the bias current. Dashed lines indicate slopes with exponential factors 1, 2, 3, respectively.

184 of magnitude, the detection probability decreases linearly (in a log scale) with the decrease of the
 185 incident power (average number of incident photons), and the probability slopes for various bias
 186 currents are well-fitted by $A \exp(-nbV)$ dependence, and are quantized. Here A and b are fitting
 187 parameters and b is the same for all three curves. This resembles the multi-photon detection [5],
 188 where for a smaller bias current ($I = 23$ nA), the slope is larger $\approx A \exp(-3bV)$ than for larger bias
 189 current $\approx A \exp(-2bV)$ for $I = 25$ nA and $\approx A \exp(-bV)$ for $I = 26$ nA.

190 Despite we see a consistent switching due to 9 GHz signal even at 23 nA, at the moment we can-
 191 not estimate the absorption efficiency, because of the uncertainty in determination of losses in the
 192 twisted pair at the frequency 9 GHz and of the absorption efficiency in the junction. Therefore
 193 we do not convert the attenuation to the power to avoid an additional insecure parameter. The ex-
 194 periments will be continued with better statistics and signal calibration to extract the number of
 195 detected photons. We expect that the sensitivity of the considered threshold detector will be de-
 196 creased in comparison with the situation without the phase diffusion, however new studies are re-
 197 quired to answer this question.

198 **Conclusions**

199 In the present work, temporal and detecting characteristics of a low critical current Al Josephson
200 junction have been studied experimentally. From measurements of switching current distributions
201 and the dark count time intervals, the operation in a phase diffusion regime is evident. It is shown
202 by comparison with the theory that the phase diffusion regime allows to significantly improve
203 noise immunity of a device, radically increasing the mean time between dark counts. However,
204 in the same way, the phase diffusion should decrease the single photon sensitivity of the considered
205 threshold detector, which will be studied in future experiments.

206 The detection probability versus attenuation voltage shows tail slopes quantization, which resem-
207 bles a few-photon detection. The use of such a device for supersensitive detection has essential ap-
208 plications. In particular, such a detector can be used in the task of searching the axions and measur-
209 ing signals generated by quantum circuits at a frequency of 6-9 GHz. In the future, it is supposed to
210 improve the measurement setup and conduct research on the detection of test signals in the range of
211 8-14 GHz.

212 **Acknowledgements**

213 The authors wish to thank G. N. Gol'tsman for discussions and critical comments.

214 **Funding**

215 The work is supported by Russian Science Foundation (Project No. 19-79-10170).

216 **References**

- 217 1. Barbieri, R.; Braggio, C.; Carugno, G.; Gallo, C. S.; Lombardi, A.; Ortolan, A.; Pengo, R.;
218 Ruoso, G.; Speake, C. C. *Phys. Dark Universe* **2017**, *15*, 135–141. doi:10.1016/j.dark.2017.
219 01.003.
- 220 2. McAllister, B. T.; Flower, G.; Ivanov, E. N.; Goryachev, M.; Bourhill, J.; Tobar, M. E. *Phys.*
221 *Dark Universe* **2017**, *18*, 67–72. doi:10.1016/j.dark.2017.09.010.

- 222 3. Kuzmin, L. S.; Sobolev, A. S.; Gatti, C.; Di Gioacchino, D.; Crescini, N.; Gordeeva, A.;
223 Il'ichev, E. *IEEE Trans. Appl. Supercond.* **2018**, *28* (7), 1–5. doi:10.1109/TASC.2018.
224 2850019.
- 225 4. Inomata, K.; Lin, Z.; Koshino, K.; Oliver, W. D.; Tsai, J.-S.; Yamamoto, T.; Nakamura, Y. *Nat.*
226 *Commun.* **2016**, *7* (12303), 1–7. doi:10.1038/ncomms12303.
- 227 5. Gol'tsman, G. N.; Okunev, O.; Chulkova, G.; Lipatov, A.; Semenov, A.; Smirnov, K.;
228 Voronov, B.; Dzardanov, A.; Williams, C.; Sobolewski, R. *Appl. Phys. Lett.* **2001**, *79* (6),
229 705–707. doi:10.1063/1.1388868.
- 230 6. Baeva, E. M.; Sidorova, M. V.; Korneev, A. A.; Smirnov, K. V.; Divochy, A. V.; Moro-
231 zov, P. V.; Zolotov, P. I.; Vakhtomin, Yu. B.; Semenov, A. V.; Klapwijk, T. M.; Khrapai, V. S.;
232 Goltsman, G. N. *Phys. Rev. Appl.* **2018**, *10* (6), 064063. doi:10.1103/PhysRevApplied.10.
233 064063.
- 234 7. Guarcello, C.; Valenti, D.; Spagnolo, B.; Pierro, V.; Filatrella, G. *Nanotechnology* **2017**, *28*
235 (13), 134001. doi:10.1088/1361-6528/aa5e75.
- 236 8. Zgirski, M.; Foltyn, M.; Savin, A.; Norowski, K.; Meschke, M.; Pekola, J. *Phys. Rev. Appl.*
237 **2018**, *10* (4), 044068. doi:10.1103/PhysRevApplied.10.044068.
- 238 9. Guarcello, C.; Braggio, A.; Solinas, P.; Giazotto, F. *Phys. Rev. Appl.* **2019**, *11* (2), 024002.
239 doi:10.1103/PhysRevApplied.11.024002.
- 240 10. Guarcello, C.; Valenti, D.; Spagnolo, B.; Pierro, V.; Filatrella, G. *Phys. Rev. Appl.* **2019**, *11*
241 (4), 044078. doi:10.1103/PhysRevApplied.11.044078.
- 242 11. Guarcello, C.; Braggio, A.; Solinas, P.; Pepe, G. P.; Giazotto, F. *Phys. Rev. Appl.* **2019**, *11* (5),
243 054074. doi:10.1103/PhysRevApplied.11.054074.
- 244 12. Anghel, D. V.; Kulikov, K.; Galperin, Y. M.; Kuzmin, L. S. *Phys. Rev. B* **2020**, *101* (2),
245 024511. doi:10.1103/PhysRevB.101.024511.

- 246 13. Wallraff, A.; Duty, T.; Lukashenko, A.; Ustinov, A. V. *Phys. Rev. Lett.* **2003**, *90* (3), 037003.
247 doi:10.1103/PhysRevLett.90.037003.
- 248 14. Oelsner, G.; Revin, L. S.; Il'ichev, E.; Pankratov, A. L.; Meyer, H.-G.; Grönberg, L.; Has-
249 sel, J.; Kuzmin, L. S. *Appl. Phys. Lett.* **2013**, *103* (14), 142605. doi:10.1063/1.4824308.
- 250 15. Oelsner, G.; Andersen, C. K.; Reháč, M.; Schmelz, M.; Anders, S.; Grajcar, M.; Hübner, U.;
251 Mølmer, K.; Il'ichev, E. *Phys. Rev. Appl.* **2017**, *7* (1), 014012. doi:10.1103/PhysRevApplied.7.
252 014012.
- 253 16. Chen, Y.-F.; Hover, D.; Sendelbach, S.; Maurer, L.; Merkel, S. T.; Pritchett, E. J.; Wil-
254 helm, F. K.; McDermott, R. *Phys. Rev. Lett.* **2011**, *107* (21), 217401. doi:10.1103/
255 PhysRevLett.107.217401.
- 256 17. Poudel, A.; McDermott, R.; Vavilov, M. G. *Phys. Rev. B* **2012**, *86* (17), 174506. doi:10.1103/
257 PhysRevB.86.174506.
- 258 18. Yu, H. F.; Zhu, X. B.; Peng, Z. H.; Cao, W. H.; Cui, D. J.; Tian, Y.; Chen, G. H.; Zheng, D. N.;
259 Jing, X. N.; Lu, L.; Zhao, S. P.; Han, S. *Phys. Rev. B* **2010**, *81* (14), 144518. doi:10.1103/
260 PhysRevB.81.144518.
- 261 19. Yu, H. F.; Zhu, X. B.; Peng, Z. H.; Tian, Y.; Cui, D. J.; Chen, G. H.; Zheng, D. N.; Jing, X. N.;
262 Lu, L.; Zhao, S. P.; Han, S. *Phys. Rev. Lett.* **2011**, *107* (6), 067004. doi:10.1103/PhysRevLett.
263 107.067004.
- 264 20. Longobardi, L.; Massarotti, D.; Rotoli, G.; Stornaiuolo, D.; Papari, G.; Kawakami, A.;
265 Pepe, G. P.; Barone, A.; Tafuri, F. *Phys. Rev. B* **2011**, *84* (18), 184504. doi:10.1103/PhysRevB.
266 84.184504.
- 267 21. Koval, Y.; Fistul, M. V.; Ustinov, A. V. *Phys. Rev. Lett.* **2004**, *93* (8), 087004. doi:10.1103/
268 PhysRevLett.93.087004.

- 269 22. Martinis, J. M.; Kautz, R. L. *Phys. Rev. Lett.* **1989**, *63* (14), 1507–1510. doi:10.1103/
270 PhysRevLett.63.1507.
- 271 23. Vion, D.; Götz, M.; Joyez, P.; Esteve, D.; Devoret, M. H. *Phys. Rev. Lett.* **1996**, *77* (16),
272 3435–3438. doi:10.1103/PhysRevLett.77.3435.
- 273 24. Grabert, H.; Ingold, G.-L.; Paul, B. *EPL* **1998**, *44* (3), 360–366. doi:10.1209/epl/
274 i1998-00480-8.
- 275 25. Franz, A.; Koval, Y.; Vasyukov, D.; Müller, P.; Schneidewind, H.; Ryndyk, D. A.; Keller, J.;
276 Helm, C. *Phys. Rev. B* **2004**, *69* (1), 014506. doi:10.1103/PhysRevB.69.014506.
- 277 26. Massarotti, D.; Longobardi, L.; Galletti, L.; Stornaiuolo, D.; Rotoli, G.; Tafuri, F. *Low Temp.*
278 *Phys.* **2013**, *39* (3), 294–298. doi:10.1063/1.4795203.
- 279 27. Likharev, K. K. *Dynamics of Josephson junctions and circuits*; Gordon and Breach Science
280 Publishers: New York, 1986.
- 281 28. Blackburn, J. A.; Cirillo, M.; Grønbech-Jensen, N. *Phys. Rep.* **2016**, *611*, 1–33. doi:10.1016/j.
282 physrep.2015.10.010.
- 283 29. Longobardi, L.; Massarotti, D.; Stornaiuolo, D.; Galletti, L.; Rotoli, G.; Lombardi, F.;
284 Tafuri, F. *Phys. Rev. Lett.* **2012**, *109* (5), 050601. doi:10.1103/PhysRevLett.109.050601.
- 285 30. Kramers, H. A. *Physica* **1940**, *7* (4), 284–304. doi:10.1016/S0031-8914(40)90098-2.
- 286 31. Hänggi, P.; Talkner, P.; Borkovec, M. *Rev. Mod. Phys.* **1990**, *62* (2), 251–341. doi:10.1103/
287 RevModPhys.62.251.
- 288 32. Caldeira, A. O.; Leggett, A. J. *Phys. Rev. Lett.* **1981**, *46* (4), 211–214. doi:10.1103/
289 PhysRevLett.46.211.
- 290 33. Malakhov, A. N.; Pankratov, A. L. *Physica C* **1996**, *269* (1), 46–54. doi:10.1016/
291 0921-4534(96)00426-1.

- 292 34. Malakhov, A. N.; Pankratov, A. L. *Wiley Online Library* **2002**, *121*, 357–438. doi:10.1002/
293 0471264318.ch6.